

Dielectric behaviour of nano-crystalline spinel $\text{Ni}_{0.2}\text{Ca}_{0.8}\text{Fe}_2\text{O}_4$ and their nano-composite with polypyrrole

ARUN S PRASAD^{†*}, S N DOLIA and P PREDEEP^{††}

Department of Physics, University of Rajasthan, Jaipur 302 004, India

[†]Arulmigu Meenakshi Amman College of Engineering, Vadamavandal 604 410, India

^{††}Laboratory for Unconventional Electronics and Photonics, National Institute of Technology, Calicut 673 601, India

MS received 15 June 2010

Abstract. The spinel ferrite nano-particles of chemical composition $\text{Ni}_{0.2}\text{Ca}_{0.8}\text{Fe}_2\text{O}_4$ have been prepared by sol-gel method. Subsequently, the nanoparticles are encapsulated with the intrinsically conducting polymer shell of polypyrrole. The X-ray diffraction patterns confirm the single phase cubic spinel structure of the materials. To understand the dielectric properties of the materials, frequency-dependent dielectric measurement has been performed at 300 K in the range of 100 MHz to 2 MHz. On polymerization, both the dielectric strength as well the dielectric loss is significantly increased. Also, the dielectric conductivity, which arises from the electron hopping mechanism, is considerably increased on polymerization.

Keywords. Nanoparticle; dielectric constant; hopping; conducting polymer.

1. Introduction

Magnetic nanoparticles of spinel ferrites having unique quantum properties like super-paramagnetism (Cullity 1972; Handdy 2000), tunnelling of magnetization (Chen *et al* 1998; Khan *et al* 2001) and spin injection (Ren *et al* 2008) are potential materials for modern electronic and biomedical applications. For such nanoparticle systems, the grain boundaries are the regions of mismatch between energy states of adjacent grains. This acts as a barrier to the flow of electrons and helps in reducing the presence of Fe^{2+} as ions like oxygen move faster in small grain sizes, and keeping iron in the Fe^{3+} state only. By virtue of this mechanism, the spinel nano-ferrites have enhanced magnetic properties and higher resistivities compared to their bulk counterparts. Functionalize such nanoparticle surfaces with functional materials like polymers are the trend in modern material research to incorporate synergic properties to the material.

Intrinsically conducting polymers (ICPs) are considered as better candidates for such functional modifications (Murillo *et al* 2004; Dey *et al* 2005; Zhang *et al* 2005). Since ICPs are not known for their mechanical properties, they are often supported on a substrate, e.g. a particle (Murillo *et al* 2004). On growing ICPs to the nano-grain surface, both the nanoparticles' and the ICPs' properties modify each other due to the interaction at molecular level. ICPs like polyaniline (PAni), polypyrrole

(PPy), etc can withstand high electrostatic fields without any dielectric breakdown. Usually PAni, PPy, etc have their maximum dielectric constant go up to 10000 (Dey *et al* 2005). In this context, an attempt has been made in this paper to analyse the structural as well as dielectric behaviour of such hybrid nano-composite materials made of $\text{Ni}_{0.2}\text{Ca}_{0.8}\text{Fe}_2\text{O}_4$ and polypyrrole.

2. Experimental

2.1 Nanoparticle synthesis

The magnetic nanoparticles of $\text{Ni}_{0.2}\text{Ca}_{0.8}\text{Fe}_2\text{O}_4$ have been synthesized by the sol-gel method. In this method, analytical-grade $\text{Ni}(\text{NO}_3)_2 \cdot 6\text{H}_2\text{O}$, $\text{Ca}(\text{NO}_3)_2 \cdot 9\text{H}_2\text{O}$, $\text{Fe}(\text{NO}_3)_3 \cdot 9\text{H}_2\text{O}$ and citric acid ($\text{C}_6\text{H}_8\text{O}_7$) were used as raw materials. The molar ratio of the nitrates to citric acid was kept 1 : 1, and all the nitrates and citric acid solutions were mixed together with continuous stirring. A small amount of ammonia was added to the solution to adjust the pH close to 7. The mixture was slowly heated to 90°C, leading to the formation of xerogels. Further heating resulted in burning of the gel in a self-propagating combustion manner until all the gel gets burnt out completely to form a loose powder.

2.2 Synthesis of NCF/PPy nano-composites

The nanoparticles of $\text{Ni}_{0.2}\text{Ca}_{0.8}\text{Fe}_2\text{O}_4$ (henceforth NCF) were then dispersed in 20 ml of de-ionized water under

*Author for correspondence (asp.physics@gmail.com)

constant ultrasonic action. A fractional, 200 ml standardized aqueous ammonium peroxodisulphate (APS) solution maintaining pyrrole : APS mole ratio 1 : 1.25, was added to the dispersion. After 30 min, pyrrole of known volume was slowly syringed into the dispersion under constant ultrasonic action. The solution was then kept under sonication for about 1 h for complete polymerization followed by centrifugation at 10000 rpm. The resulting composite came out as black solid residue, which was washed thoroughly first with ethyl alcohol and then with de-ionized water several times to remove all the adhering impurities, followed by drying overnight in a vacuum oven at 50°C. The nano-composite sample obtained was denoted as NCFPPy.

3. Results and discussion

Figure 1(a) shows the powder X-ray diffraction pattern of the pristine NCF sample. The Bragg reflections are indexed and the cell parameters are refined using PDP11.1 Program (Calligaris *et al* 1990). The estimated cell constant, a is 8.42 Å, which is closer to that of the nanoparticles of Fe_3O_4 , i.e. 8.39 Å (Chikazumi *et al* 1978; Krupica *et al* 1982). This confirms the single phase cubic spinel structure of the nanoparticles of $\text{Ni}_{0.2}\text{Ca}_{0.8}\text{Fe}_2\text{O}_4$ without the presence of iron oxide phases. Also, considerably broadened peaks in the XRD pattern are indicative of the presence of nano-sized particles. Using the (311) reflection peak in the XRD pattern, the average crystallite size, t , is estimated with the help of Debye–Sherrer equation (Cullity 1959)

$$t = \frac{0.9\lambda}{B \cos \theta_B}; \quad B = (B_M^2 - B_S^2)^{1/2}, \quad (1)$$

where λ is the X-ray wavelength, θ_B the Bragg angle of reflection, B_M the broadening (in radians) of diffraction

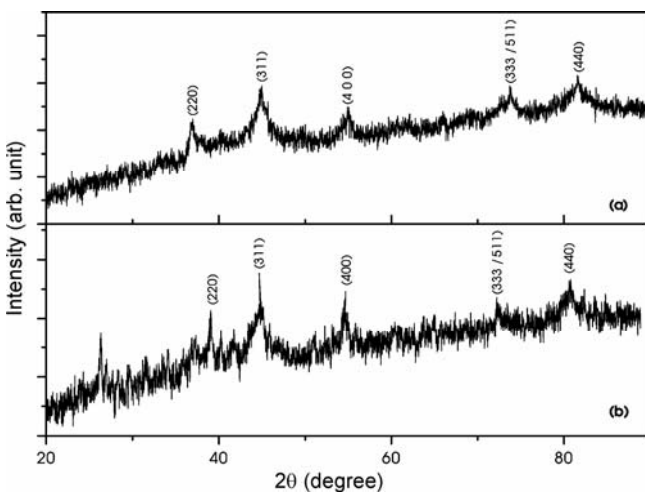


Figure 1. X-ray diffraction patterns of (a) pristine NCF nanoparticles and (b) NCFPPy nanocomposite.

line measured at half of its maximum intensity and B_S the broadening (in radians) in a reflection at about the same Bragg angle in a standard bulk crystallite sized sample (silicon). Use of this equation yields an average crystallite size of 8 nm for NCF sample.

Figure 1(b) represents the XRD pattern obtained for NCFPPy sample, where all the characteristic peaks obtained for pristine NCF are reproduced. Nevertheless, the amorphous broad peak ($2\theta = 26.31^\circ$) is related to the polymeric shell in the nanoparticles (Murillo *et al* 2004; Dey *et al* 2005; Zhang *et al* 2005). The average crystallite size evaluated is 10 nm and the crystal growth could be attributed to the polymerization process. The estimated cell constant also increases to 8.450 Å after polymerization.

3.1 Dielectric and transport properties

Figure 2 shows the variation of dielectric constant (ϵ'_r) with frequency for NCF and NCFPPy samples, respectively, at 300 K. Systematically, for the two samples, the value of ϵ'_r decreases with frequency in a normal manner as observed by Rezlescu and Rezlescu (1974) and explained on the basis of available ferrous ions on octahedral sites. Since Fe^{2+} ions preferentially occupy the B site, A–A hopping is considered to be not taken place. Moreover, as the B–B distance is smaller than A–B distance, electron hopping between B–B ions is assigned as the main mechanism of conduction. As a consequence, it is possible for these ions to be polarized to maximum possible extent at the octahedral site. Further, as the frequency of externally applied electric field increases, although the same number of ferrous ions is present in the ferrite material, the dielectric constant (ϵ'_r) decreases; because beyond certain frequency of applied electric field, the electronic exchange between the ferrous and ferric ions, i.e. $\text{Fe}^{2+} \leftrightarrow \text{Fe}^{3+}$, cannot follow the alternating field.

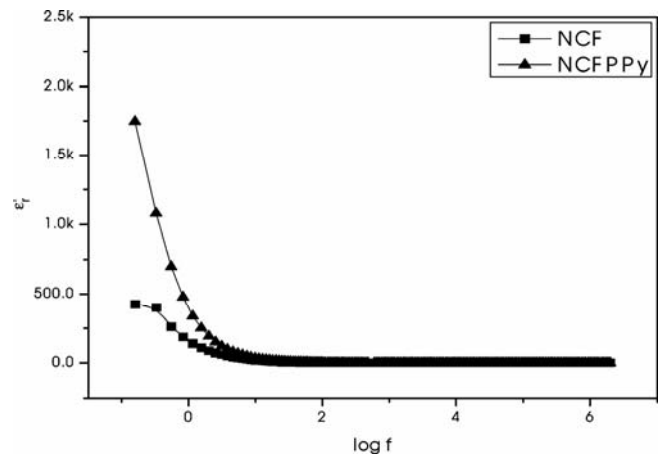


Figure 2. Variation of dielectric constant (ϵ'_r) as a function of log frequency for pristine NCF and NCFPPy samples at 300 K.

The maximum value of dielectric constant at 100 mHz for the pristine NCF sample is 425, whereas that for NCFPPy samples is 1747. The increase in the value of dielectric constant (ϵ'_r) for the nano-composite samples is attributed to the coating effectiveness. However, from the polymer part, the perspective is reverse: the value gets reduced (Dey *et al* 2005). This is because the presence of nanoparticle reduces the polymer chain length.

Figure 3 shows the variation of the imaginary part of dielectric constant, i.e. dielectric loss (ϵ''_r), with frequency for NCF and NCFPPy, respectively, at 300 K. From the plot, it is understood that the numerical value of the dielectric loss decreases with increase in frequency for all the three samples. The decrease in ϵ''_r with increase in frequency is observed and agreed well with Debye's type relaxation process (Kobayashi 1986). The loss is significantly large for the nano-composite samples compared to that of pristine NCF sample.

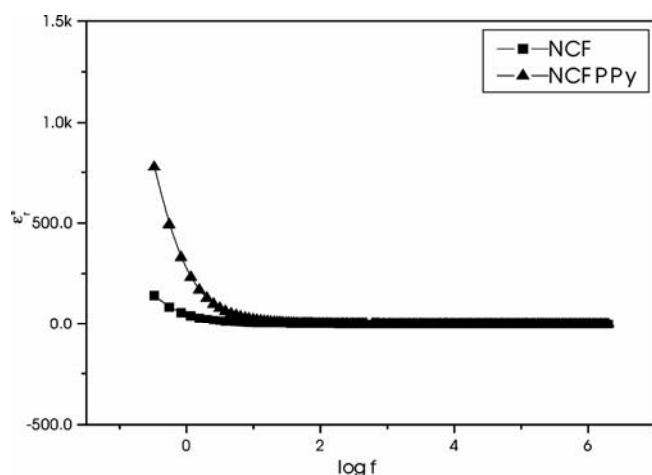


Figure 3. Variation of the numerical value of dielectric loss (ϵ''_r) as a function of log frequency for pristine NCF and NCFPPy samples at 300 K.

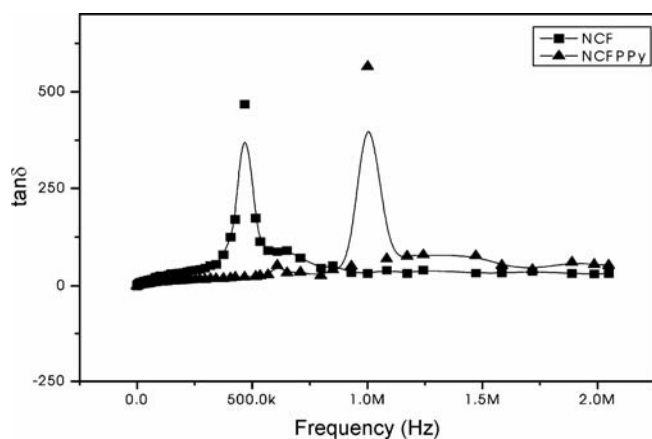


Figure 4. Variation of the loss tangent ($\tan \delta$) as a function of frequency for pristine NCF and NCFPPy samples at 300 K.

Figure 4 shows the variation of the loss tangent ($\tan \delta$) with frequency of pristine NCF and NCFPPy samples at 300 K. For the pristine sample, NCF, the $\tan \delta$ shows a maximum at 0.47 MHz. A qualitative explanation can be given for the occurrence of the maximum in the $\tan \delta$ vs frequency curves as pointed out by Iwauchi (1971), i.e. when the hopping frequency is nearly equal to that of the frequency of externally applied electric field, a maximum of loss tangent will be observed. In the case of nano-composite, the peaks obtained for such a maxima are shifted towards the higher-frequency region, indicative of the increased loss suffered after polymerization. For the NCFPPy sample, the maximum loss tangent is observed at 1 MHz.

The shift of peaks towards the higher-frequency region, in the case of nano-composite sample, can be explained on the basis of the jumping or hopping probability of electrons per unit time (Debye 1929). The condition for observing a maximum in the dielectric losses of a dielectric material is $w\tau = 1$, where w is the $2\pi f_{\max}$ and τ the relaxation time. Now the relaxation time τ is related to the jumping probability per unit time p , by the equation $\tau = 1/2 p$ or $f_{\max} \propto p$. This shows that f_{\max} is proportional to the jumping or hopping probability. Now, an increase of f_{\max} for nano-composites indicates that the hopping or jumping probability increases with polymer coating. This can be more clearly understood from the conductivity graph.

Figure 5 shows the variation of logarithmic conductivity with logarithmic frequency for NCF and NCFPPy samples, respectively. This can be explained with the help of Maxwell-Wagner two layer model or heterogeneous model of the polycrystalline structure of ferrites (Koops 1951). As the frequency of the applied field increases, the conductive layer become more active by promoting the hopping of electron between Fe^{2+} and Fe^{3+} ions, thereby

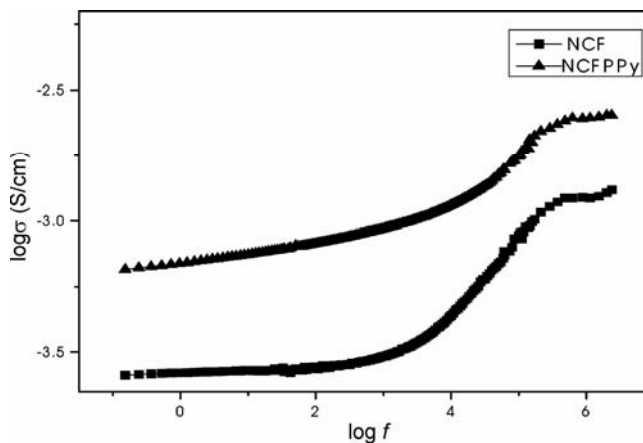


Figure 5. Variation of the logarithmic conductivity with log frequency of pristine NCF and NCFPPy samples at 300 K.

increasing the hopping frequency. Thus, we observed a gradual increase in conductivity with frequency. However, in the nano-composites, the surface coating also contributes to the hopping mechanism and thereby the conductivity increases. The conductivity obtained at 2 MHz is of the order of 10^{-3} Scm^{-1} for the pristine as well the PPy-coated samples. In the case of NCF, the value is $1.3 \times 10^{-3} \text{ Scm}^{-1}$ and for NCFPPy the value is $2.5 \times 10^{-3} \text{ Scm}^{-1}$.

4. Conclusions

The nanoparticles of $\text{Ni}_{0.2}\text{Ca}_{0.8}\text{Fe}_2\text{O}_4$ are prepared by the sol-gel method and are encapsulated with polypyrrole using chemical oxidative polymerization technique. The broadening of XRD peaks gives an average crystallite size of 8 nm for NCF sample using Debye Scherrer equation. The presence of the amorphous peak at $2\theta = 26.31^\circ$, along with all the characteristic peaks of pristine ferrites confirm the formation of core shell structure. From dielectric measurement, it has been found that the dielectric constant shows a normal reduction with frequency. The value of dielectric constant is substantially increased from 425 to 1747 at 100 mHz on polymerization. Also, the increase in loss factor is due to the eddy current loss, which in turn is responsible for the increase in conductivity after polymerization. The value is in the order of $10^{-3} \text{ S cm}^{-1}$ at 2 MHz.

References

- Calligaris M and Geremia S 1990 *Powder diffraction package version 11.1*, Dipartimento di science chimiche, universita di Trieste
- Chen Q and Zhang J Z 1998 *Appl. Phys. Lett.* **73** 3156
- Chikazumi S and Charap S H 1978 *Physics of magnetism* (ed.) E Robert (Florida: Kreiger Pub. Co)
- Cullity B D 1959 *Elements of X-ray diffraction* (Reading: Addison Wesley)
- Cullity B D 1972 *Introduction to magnetic materials* (USA: Addison Wesley Pub. Co.)
- Debye P 1929 *Polar molecules* (New York: Chemical Catalogue Company)
- Dey A, De A and De S K 2005 *J. Phys.: Condens. Matter* **17** 5895
- Handy R G O 2000 *Modern magnetic materials: principle and application* (USA: John Wiley and Sons, Inc.)
- Iwachi K 1971 *Jap. J. Appl. Phys.* **10** 1520
- Kahn M L and Zhang J Z 2001 *Appl. Phys. Lett.* **78** 3651
- Kobayashi M, Akishinge Y and Sawaguchi E 1986 *J. Phys. Soc. Japan* **55** 4044
- Koops C 1951 *Phys. Rev.* **38** 216
- Krupicka S and Novak P 1982 in *Ferromagnetic materials* (ed.) E P Wholfarth (Amsterdam: North Holland Pub. Co.) **Vol III**
- Murillo N, Ochoteco E, Alesanco Y, Pomposo J A, Rodriguez J, Gonzalez J, del Val J J, Gonzalez J M, Britel M R, Varela-Feria F M and de Arellano-Lopez A R 2004 *Nanotechnology* **15** S322
- Ren J, Zhang Y and Xie S 2008 *Organic Electronics* **9** 1017
- Rezlescu N and Rezlescu E 1974 *Phys. Status Solidi* **A23** 575
- Zhang Z, Wan M and Wei Y 2005 *Nanotechnology* **16** 2827